A hybrid method for determining the reluctivity tensor components of Goss textured ferromagnetic materials

Received September 2002
Revised January 2003
Accepted April 2003

Hans Vande Sande
Flanders' Mechatronics Technology Centre, Heverlee-Leuven, Belgium
François Henrotte and Kay Hameyer
Department of ESAT, Div. ELECTA, Katholieke Universiteit Leuven, Heverlee-Leuven, Belgium
Ludo Froyen
Department of MTM, Katholieke Universiteit Leuven, Heverlee-Leuven, Belgium

Keywords *Ferroelectricity, Magnetic fields, Silicon, Electromagnetic fields*

Abstract *For anisotropic materials, the magnetic field vector $\vec{H}$ and the flux density vector $\vec{B}$ are parallel with each other only along a few distinct directions. When performing unidirectional measurements, only the component of $\vec{B}$ along the direction under consideration is measured. It is not possible to deduce the angle between $\vec{B}$ and $\vec{H}$ from unidirectional measurements alone. For ferromagnetic materials having a Goss-texture, as most transformer steels have, this paper demonstrates a way to compute this angle a posteriori, by the combination of measurements with a physical anisotropy model.*

1. Introduction

It is customary in computational electromagnetics to directly implement material characteristics in the form given by the steel manufacturers. As the measurements of such characteristics involve generally only scalar quantities, their implementation as such in a magnetic field finite element program constitutes a *de facto* generalisation, which is not supported by any arguments and never mentioned. Measurements give only a partial view on the complicated behaviour of matter (and in particular that of iron

This is a revised and enhanced version of a paper which was originally presented as a conference contribution at the *XII Symposium on Electromagnetic Phenomena in Nonlinear Circuits (EPNC)*, held in Leuven, Belgium, on 1-3 July 2002. This is one of a small selection of papers from the Symposium to appear in the current and future issues of *COMPEL*.
The authors are grateful to the Belgian "Fonds voor Wetenschappelijk Onderzoek Vlaanderen" (project G.0420.99) and the Belgian Ministry of Scientific Research (IUAP No. P5/34).

COMPEL: The International Journal for Computation and Mathematics in Electrical and Electronic Engineering
Vol. 23 No. 2, 2004
pp. 579-589

0332-1649
DOI 10.1108/03321640410510767

and steel). They therefore need to be interpreted in the context of the mechanisms in play at the microscopic level. The purpose of this paper is to propose such an interpretation in the case of the analysis of the anisotropy of laminated steels.

Unidirectional magnetic measurement setups measure the components of both, the magnetic flux density $\vec{B}$ (T) and the magnetic field strength $\vec{H}$ (A/m) along a fixed direction. They can be used to assess the anisotropy of a ferromagnetic material, by measuring the magnetisation curves $B_{\text{meas}}(H_{\text{meas}}, \alpha)$ of a series of small strips, cut out of a metal sheet under various angles. The reluctivity ν_{meas} (A m/V s), defined by

$$\nu_{\text{meas}} = \frac{H_{\text{meas}}}{B_{\text{meas}}}, \tag{1}$$

depends non-linearly on B_{meas} and α. Figure 1 shows the measured reluctivity curves for a conventional grain-oriented (CGO) steel Fe-Si 3 per cent, along a number of directions with respect to the rolling direction (RD) (Shirkoohi and Arikat, 1994; Shirkoohi and Liu, 1994).

2. Goss-texture

From Figure 1, it follows that the material is the easiest to magnetise along the rolling direction, while it is the hardest to magnetise at an angle of approximately 55° with respect to the rolling direction. These characteristics reveal the Goss-texture of the steel sheet. Silicon steel, mainly composed of cubic iron crystals, can be given a Goss-texture by an appropriate manufacturing process requiring several rolling stages and annealing phases in the presence of inhibitors (Lee and Jeong, 1998; Takahashi *et al.*, 1996). A silicon steel sheet features a Goss-texture when for all crystals the ⟨001⟩ axis coincides with the rolling direction and the {110} plane is parallel to the surface of the sheet (Figure 2). The behaviour observed in Figure 1 can be explained by thoroughly considering the magnetisation process.

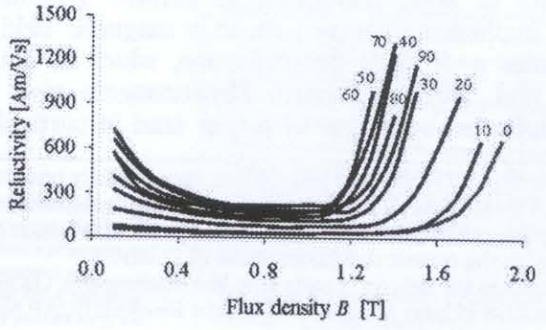

Figure 1.
The reluctivity curves for CGO steel (FeSi 3 per cent), under various angles with respect to the RD

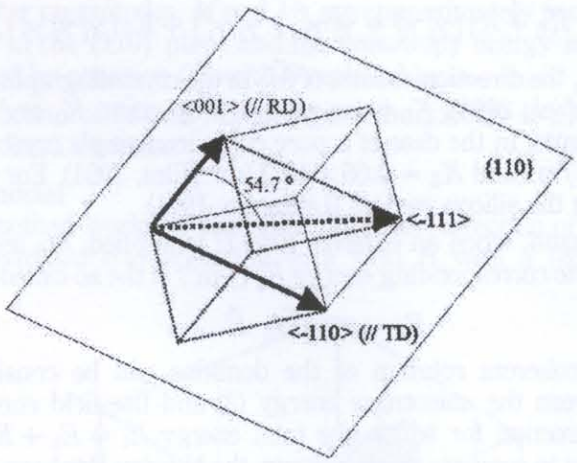

Figure 2.
Definition of a Goss-texture, with the RD and the transverse direction (TD)

3. Magnetisation process

All ferromagnetic materials are characterised by the presence of magnetic domains, in which the material is magnetised up to the saturation magnetisation M_s. For a pure iron single crystal, $M_s = 1.71 \times 10^6$ A/m (Jiles, 1991). For electrical steel, its value slightly depends on the silicon content (Littmann, 1971). If no external field is applied, the magnetic domains are randomly distributed with their magnetisation vector along one of the preferred easy axes ⟨100⟩, ⟨010⟩ or ⟨001⟩. When the external field is increased slightly, the domains that are aligned in a direction close to that of the applied field start growing. At moderate fields, the domains suddenly and irreversibly rotate towards the easy axis closest to the applied field. Once they are all parallel, i.e. above the knee of the magnetisation curve, they rotate reversibly towards the applied field (Bozorth, 1951; Jiles, 1991; Robert, 1987).

This paper focuses on the latter process, often called *coherent rotation*. At those high field strengths, the domain wall motion is less important when compared to the domain rotation. It is therefore assumed that the domain walls do not move, regardless of the applied field. In this case, the magnetisation process is described in terms of anisotropy and field energies.

4. Anisotropy and field energy

Within a single domain, the magnetisation vector is denoted by $\vec{M}_d$ (A/m). Its magnitude is constant and equals M_s. Its direction depends on the direction and the magnitude of the externally applied field $\vec{H}$.

$\vec{M}_d$ naturally tends to align with one of the easy axes of the crystal. Deviation from this equilibrium state corresponds to an energy increase, which is due to the intrinsic anisotropy of the crystal. For cubic crystal systems, the *anisotropy energy* E_a (J/m^3) is given by

$$E_a = K_0 + K_1(\gamma_1^2\gamma_2^2 + \gamma_2^2\gamma_3^2 + \gamma_3^2\gamma_1^2) + K_2(\gamma_1^2\gamma_2^2\gamma_3^2), \quad (2)$$

with γ_1, γ_2 and γ_3, the direction cosines of $\vec{M}_d$ in the crystallographic coordinate system (Rollett *et al.*, 2001). K_0 is an arbitrary constant. K_1 and K_2 are the anisotropy constants. In the case of a pure cubic iron single crystal, these are $K_1 = 0.48 \times 10^5\,\mathrm{J/m^3}$ and $K_2 = 0.05 \times 10^5\,\mathrm{J/m^3}$ (Jiles, 1991). For steels, their values depend on the silicon content (Littmann, 1971).

On the other hand, when an external field $\vec{H}$ is applied, $\vec{M}_d$ tends to align with it as well. The corresponding energy E_h ($\mathrm{J/m^3}$) is the so-called *field energy*

$$E_h = -\mu_0 \vec{M}_d \cdot \vec{H}. \quad (3)$$

The process of coherent rotation of the domains can be considered as a competition between the anisotropy energy (2) and the field energy (3): $\vec{M}_d$ stabilises in a direction for which the total energy $E_t = E_a + E_h$ attains a minimum. In order to compute this minimum, the Newton-Raphson method can be applied (Rollett *et al.*, 2001).

In practice, the ⟨001⟩ direction and the RD can differ slightly (Nakano *et al.*, 1999). In the model presented here, it is assumed that they are in parallel. The measurement setup generates a field in the {110} plane. If the angle α between $\vec{H}$ and the ⟨001⟩ direction is smaller than 54.7°, the local magnetisation vector $\vec{M}_d$ lies in the {110} plane as well. In that case, equations (2) and (3) simplify into

$$E_a = \frac{K_1}{4}\sin^2\theta(4 - 3\sin^2\theta) + \frac{K_2}{4}\cos^2\theta\sin^4\theta \quad (4)$$

and

$$E_h = -\mu_0 M_s |\vec{H}| \cdot \cos(\alpha - \theta), \quad (5)$$

where θ is the angle between $\vec{M}_d$ and the ⟨001⟩ (//RD) direction. On the other hand, if $\alpha > 54.7°$, $\vec{M}_d$ tries to align with one of the easy axes that are not in the {110} plane. Since attraction to the ⟨100⟩ axis and the ⟨010⟩ axis is of the same probability, it is obvious that all individual vectors $\vec{M}_d$, when superposed, yield a global magnetisation vector $\vec{M}$ that lies in the {110} plane.

For the analysis of CGO steel with 3 per cent Si, $M_s = 1.61 \times 10^6\,\mathrm{A/m}$ and $K_1 = 0.375 \times 10^5\,\mathrm{J/m^3}$ (Littmann, 1971). The influence of K_2 on E_a is neglected. The anisotropy energy, computed in the stable positions of $\vec{M}_d$, is plotted in Figure 3 as a function of the applied field $|\vec{H}|$ and its direction α. For the same data, Figure 4 shows the angle θ between the global magnetisation vector $\vec{M}$ and the ⟨001⟩ axis. Several conclusions can be drawn from these figures:

- If α is small, $\vec{M}$ and $\vec{M}_d$ take up a position in the {110} plane close to the ⟨001⟩ axis.
- If α is close to 90°, θ is close to 90° as well. $\vec{M}$ lies in the {110} plane. However, Figure 3 reveals that $\vec{M}_d$ is not in the {110} plane if $|\vec{H}| < 35\,\mathrm{kA/m}$, because E_a varies there.

- For higher magnitudes, $\vec{M}$ and $\vec{M}_d$ are approximately parallel to $\vec{H}$. They both lie in the {110} plane and the anisotropy energy is approximately described by equation (4), with θ replaced by α.
- The direction of $\vec{M}$ and $\vec{M}_d$ changes continuously if $|\vec{H}|$ varies in time along a fixed direction.

5. Hybrid model

The hybrid method works in two steps. First, the direction of $\vec{M}$ in the {110} plane is determined corresponding to a field $\vec{H}$ with a fixed direction as

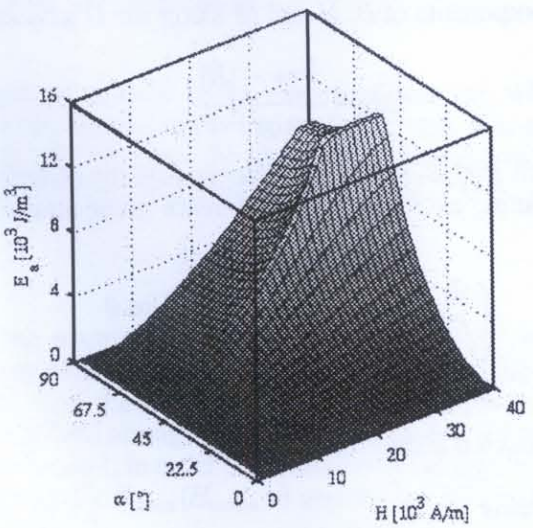

Figure 3.
The anisotropy energy computed in the stable positions of the local magnetisation vector, as a function of the magnitude and the direction of the applied field

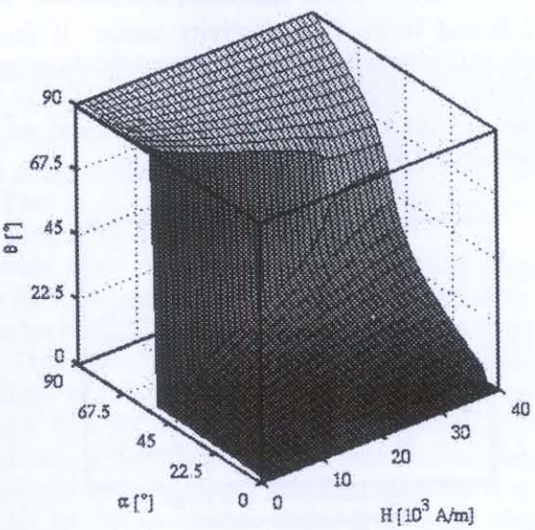

Figure 4.
The angle between the global magnetisation vector in the {110} plane and the ⟨001⟩ axis as a function of the magnitude and the direction of the applied field

discussed earlier. To accelerate the procedure, the minimum of E_t is determined by equations (4) and (5) if $\alpha < 54.7°$. Else, it is determined by equations (2) and (3) (Rollett *et al.*, 2001).

The second step is the extraction of the magnitude of $\vec{M}$ in a known direction, using the measurement data. The flux density $\vec{B}$ is related to the applied field $\vec{H}$ and the magnetisation $\vec{M}$ by:

$$\vec{B} = \mu_0(\vec{H} + \vec{M}). \tag{6}$$

Figure 5 indicates how equation (6) is related to the measurement setup. It follows that the components of $\vec{B}$, $\vec{H}$ and $\vec{M}$ along the $\vec{H}$ axis satisfy

$$|\vec{M}| = \frac{\frac{B_{meas}}{\mu_0} - |\vec{H}|}{\cos(\alpha - \theta)}. \tag{7}$$

Only $\vec{M}$ is unknown in this equation. Subsequently, the components of $\vec{B}$ are obtained by considering equation (6) in a reference frame attached to the $\langle 001 \rangle$ direction:

$$\begin{cases} \frac{|\vec{B}|}{\mu_0}\cos\beta = |\vec{H}|\cos\alpha + |\vec{M}|\cos\theta \\ \frac{|\vec{B}|}{\mu_0}\sin\beta = |\vec{H}|\sin\alpha + |\vec{M}|\sin\theta \end{cases}, \tag{8}$$

with β the angle between $\vec{B}$ and the $\langle 001 \rangle$ axis.

6. Reluctivity tensor

Using the previously presented hybrid approach, it is possible to compute the two components of $\vec{B}$ and hence the reluctivity tensor. If this symmetrical second-order tensor is considered in its principal coordinate system, it has zero off-diagonal entries (Nye, 1985). For this application, the $\langle 001 \rangle$ (//RD) and the $\langle -110 \rangle$ (//TD) axis are the principal axes of the tensor, as $\vec{B}$ and $\vec{H}$ are parallel in these directions. As a consequence,

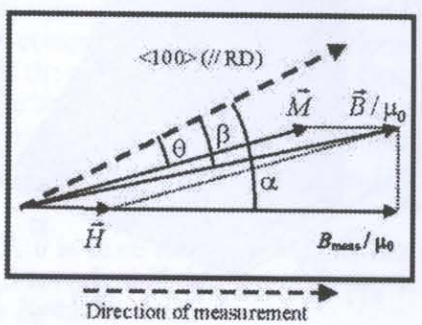

Figure 5.
The definition of the applied field, the global magnetisation vector, the flux density and their directions in relation to the measurement setup

$$\begin{pmatrix} H_{RD} \\ H_{TD} \end{pmatrix} = \begin{pmatrix} \nu_{RD} & 0 \\ 0 & \nu_{TD} \end{pmatrix} \begin{pmatrix} B_{RD} \\ B_{TD} \end{pmatrix}, \tag{9}$$

with

$$\nu_{RD} = \frac{|\vec{H}|\cos\alpha}{|\vec{B}|\cos\beta} \quad \nu_{TD} = \frac{|\vec{H}|\sin\alpha}{|\vec{B}|\sin\beta} \tag{10}$$

for a specified point of measurement.

7. Data set

Now, the analysis is applied to an empirical data set, which matches the observed anisotropic behaviour in Figure 1. For that, it is supposed that the Fröhlich-Kennely relation gives the shape of all magnetisation curves at field strengths higher than 300 A/m (Bozorth, 1951; Jiles, 1991):

$$M = M_s \frac{\zeta H}{1 + \zeta H}. \tag{11}$$

Depending on the magnetisation angle, the flux density is multiplied by a factor, which expresses the fact that the magnetisation is the easiest in the RD, harder in the TD and the hardest for $\alpha = 54.7°$. Moreover, the analysis has been carried out at field strengths higher than those used while measuring the data depicted in Figure 1, in order to demonstrate the high field characteristics. The explanatory graph $B_{meas}(H_{meas}, \alpha)$ applied for the analysis is plotted in Figure 6 ($\zeta = 8 \times 10^{-4}$).

8. Analysis

The direction β and the resulting flux density $|\vec{B}|$, computed from the empirical data set of Figure 6, are shown in Figures 7 and 8, respectively. Obviously, Figure 7 shows that for small $|\vec{H}|$, $\vec{B}$ stays close to the $\langle 001 \rangle$ (// RD) or the $\langle -110 \rangle$ (// TD) axis, irrespective of its direction α. For higher fields, $\vec{B}$ and $\vec{H}$ tend to align. This is in correspondence with the theory of magnetisation (Bozorth, 1951; Jiles, 1991; Robert, 1987).

Figure 8 reveals that, for constant $|\vec{H}|$, the actual magnitude of $\vec{B}$ does not behave like its measured component. The discontinuity which occurs for $\alpha = 54.7°$ indicates that the total energy function has local minima at lower field strengths. This reveals an interesting feature, since $\vec{B}$ may point in two different directions for that angle. Hence, $\vec{B}$ must behave differently for right-turning and left-turning fields, once α passes 54.7°. Unidirectional measurements do not allow the analysis of that kind of behaviour.

When the data shown in Figures 7 and 8 are combined, with $|\vec{H}|$ and α as a parameter, it can be observed that there is a large empty region in the

$|\vec{B}|$-β-plane (Figure 9). In order to flip over the 54.7°-direction, $\vec{B}$ must follow a contour in the empty region in a particular way. Obviously, this region is empty due to the fact that only the coherent rotation is considered. To avoid this, the model must be extended in such a way that it considers the low field behaviour and the statistical distribution of the cubic crystal orientations in the sheet as well (Fulmek and Hauser, 1996; Rollett *et al.*, 2001; Salz and Hempel, 1992). Figure 9 can be used to reveal how $\vec{H}$ behaves when $\vec{B}$ rotates in space with a constant magnitude. The result, for $|\vec{B}| = 1.55\,\mathrm{T}$, is plotted in Figure 10,

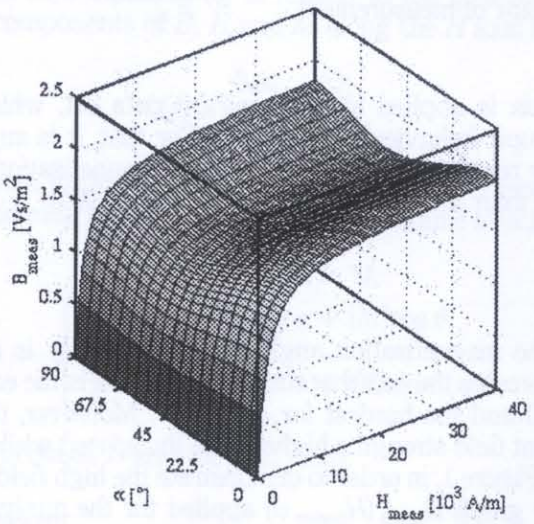

Figure 6.
The empirical data set applied to explain the hybrid anisotropy model

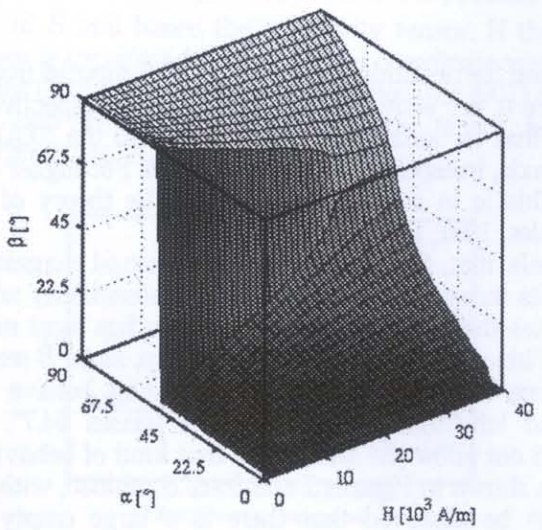

Figure 7.
The angle between the flux density vector in the {110} plane and the ⟨001⟩ axis as a function of the magnitude and the direction of the applied field

but it can be generalised to arbitrary $\vec{B}$-loci in space. This will be studied in ongoing work.

9. Conclusions

In order to assess the magnetic anisotropy of a material with a unidirectional measurement setup, the magnetisation curves must be measured in various directions of $\vec{H}$. However, this does not yield any information about the angle between $\vec{B}$ and $\vec{H}$. For Goss-textured ferromagnetic materials, a hybrid method is described that allows computing this angle at field levels for which the material saturates. The direction of $\vec{M}$ is determined by minimising the sum of

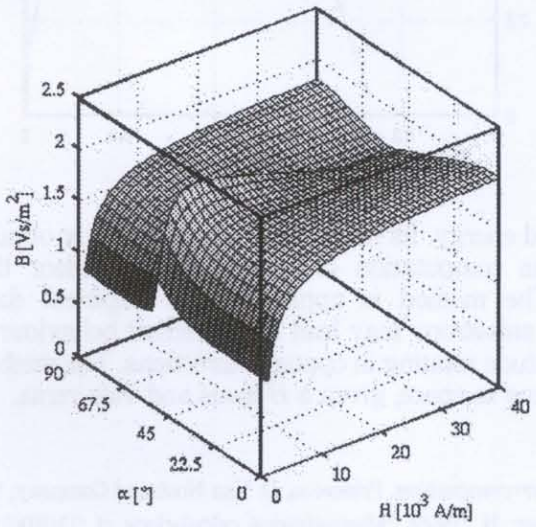

Figure 8.
The magnitude of the flux density vector in the {110} plane as a function of the magnitude and the direction of the applied field

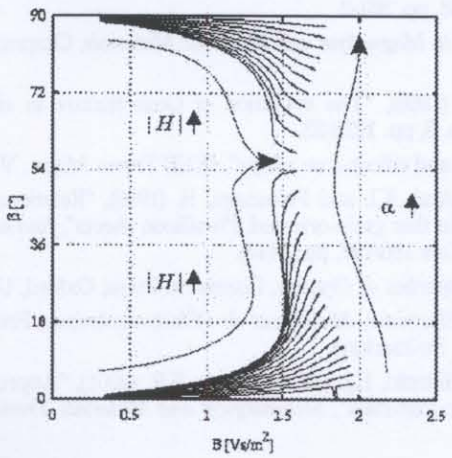

Figure 9.
Lines of constant α in the $\vec{B} - \beta$ plane, with parameter $|\vec{H}|$

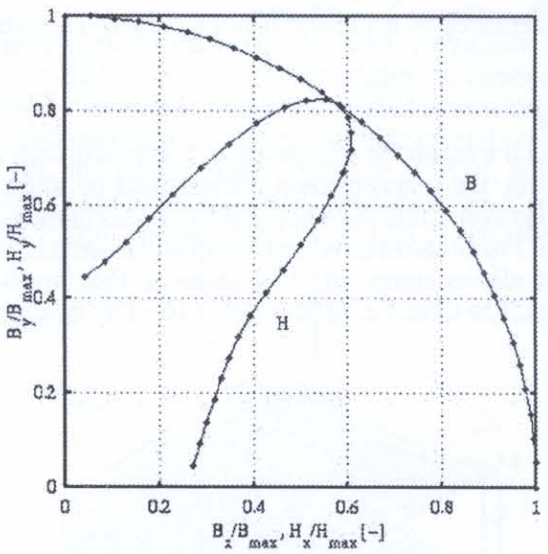

Figure 10.
The resulting $\vec{H}$-locus, when $\vec{B}$ rotates with a constant magnitude of 1.55 T

anisotropy and field energy. Its magnitude is subsequently obtained from the measurements. The computation of the reluctivity tensor then becomes straightforward. The method is applied to an empirical data set. It is demonstrated that anisotropy may lead to a different behaviour against field with a small magnitude rotating in opposite directions. The method permits to determine the $\vec{B}$-locus in space, given a $\vec{H}$-locus and vice versa.

References

Bozorth, R.M. (1951), *Ferromagnetism*, Princeton, D. Van Nostrand Company, New Jersey.

Fulmek, P.L. and Hauser, H. (1996), "Magnetisation calculations of (110)[001] FeSi sheets in different directions by statistical domain behaviour", *Journal of Magnetism and Magnetic Materials*, Vol. 157-158, pp. 361-2.

Jiles, D. (1991), *Introduction to Magnetism and Magnetic Materials*, Chapman and Hall, London, UK.

Lee, D.N. and Jeong, H.T. (1998), "The evolution of Goss texture in silicon steel", *Scripta Materialia*, Vol. 38 No. 8, pp. 1219-23.

Littmann, M.F. (1971), "Iron and silicon-iron alloys", *IEEE Trans. Magn.*, Vol. 7 No. 1, pp. 48-60.

Nakano, M., Ishiyama, K., Arai, K.I. and Fukunaga, H. (1999), "Relationship between rolling direction and texture in thin grain-oriented 3% silicon sheets", *Journal of Magnetism and Magnetic Materials*, Vols 196/197, pp. 344-5.

Nye, J.F. (1985), *Physical Properties of Crystals*, Clarendon Press, Oxford, UK.

Robert, P. (1987), *Traité d'Electricité, Matériaux de l'Électrotechnique*, Presses Polytechniques Romandes, Lausanne, Switzerland.

Rollett, A.D., Storch, M.L., Hilinski, E.J. and Goodman, S.R. (2001), "Approach to saturation in textured soft magnetic materials", *Metallurgical and Materials Transactions A*, Vol. 32A No. 10, pp. 2595-603.

Salz, W. and Hempel, K.A. (1992), "A two-dimensional model describing the magnetic behaviour of textured steel sheet", *Journal of Magnetism and Magnetic Materials*, Vol. 112 Nos 1-3, pp. 123-4.

Shirkoohi, G.H. and Arikat, M.A.M. (1994), "Anisotropic properties in high permeability grain-oriented 3.25% Si-Fe electrical steel", *IEEE Trans. Magn.*, Vol. 30 No. 2, pp. 928-30.

Shirkoohi, G.H. and Liu, J. (1994), "A finite element method for modelling of anisotropic grain-oriented steels", *IEEE Trans. Magn.*, Vol. 30 No. 2, pp. 1078-80.

Takahashi, N., Suga, Y. and Kobayashi, H. (1996), "Recent developments in grain-oriented silicon steel", *Journal of Magnetism and Magnetic Materials*, Vol. 160, pp. 98-101.